DMD Fast Forward. Published on July 18, 2011 as doi:10.1124/dmd.111.040915

Brain Regional Pharmacokinetics of p-Aminosalicylic Acid and its N-acetylated Metabolite: In Relation to Their Effectiveness in Chelating Brain Manganese

Lan Hong, Wendy Jiang, Hao Pan, Yueming Jiang, Su Zeng and Wei Zheng

Author Affiliations:

School of Health Sciences, Purdue University, West Lafayette, IN 47907, USA (L.H., W.J., W.Z.)

College of Pharmaceutical Sciences, Zhejiang University, Hangzhou 310058, China (L.H., H.P., S.Z.)

Department of Occupational Health and Toxicology, Guangxi Medical University, Nanning 530021, China (Y.M.J.)

DMD Fast Forward. Published on July 18, 2011 as DOI: 10.1124/dmd.111.040915
This article has not been copyedited and formatted. The final version may differ from this version.

a.) Running Title:

Pharmacokinetics of PAS and AcPAS in Rats

b.) Corresponding Authors:

Wei Zheng, Ph.D.
Professor and Head
School of Health Sciences, Purdue University
550 Stadium Mall Drive, Room 1169
West Lafayette, IN 47907
Phone: 765 496-6447; Fax: 765 496-1377; E-mail: wzheng@purdue.edu

c.) Page and Word Count:

Text Pages (including references, figure legends and table): 26
Tables: 2
Figures: 4
References: 33
Abstract: 213 words
Introduction: 636 words
Discussion: 1149 words

d.) Non-standard Abbreviations:

AcPAS: N-acetyl-4-amino-2-hydroxybenzoic acid
ANOVA: analysis of variance
5-ASA: 5-amino-2-hydroxybenzoic acid
$AUC_{0-\infty}$: area under the concentration-time curve from time zero to infinity
C_{max}: maximal plasma concentration after dosing
CSF: Cerebrospinal fluid
EDTA: ethylene-diamine-tetra-acetic acid
$F_{unbound}$: Fraction unbound
HPLC: high-performance liquid chromatography
Mn: manganese
MRT: mean residence time
PAS: 4-amino-2-hydroxybenzoic acid
PMSF: phenylmethylsulfonyl fluoride
TEMED: tetramethyl-ethylenediamine
T_{max}: time to reach C_{max}

DMD Fast Forward. Published on July 18, 2011 as DOI: 10.1124/dmd.111.040915
This article has not been copyedited and formatted. The final version may differ from this version.

Abstract

Para-aminosalicylic acid (PAS), an anti-tuberculosis drug in use since the 1950s, has recently been suggested to be an effective agent for treatment of manganese (Mn)-induced parkinsonian disorders. However, the neuro-pharmacokinetics of PAS and its metabolite N-acetyl-para-aminosalicylic acid (AcPAS) are unknown. This study was designed to investigate the pharmacokinetics of PAS and its distribution in brain to help better design the dosing regimen for clinical trials. Male Sprague-Dawley rats received single femoral artery injections of PAS (200mg/kg). Plasma, cerebrospinal fluid (CSF), and brain tissues were collected, and PAS and AcPAS concentrations were quantified by HPLC. Following administration, the concentrations of PAS declined rapidly in plasma with an elimination $t_{1/2}$ of 34 min; the metabolite AcPAS was detected in plasma and eliminated with a $t_{1/2}$ of 147 min. Both PAS and AcPAS were detected in brain tissues; AcPAS had a much higher tissue concentration and a longer $t_{1/2}$ than the parent PAS in most tissues examined. While both were present in blood or tissues as free, unbound molecules, AcPAS appeared to have a higher tissue affinity than PAS. Taken together, our results suggest that a dosing regimen with continuous iv infusion of PAS is necessary to achieve therapeutic levels in targeted brain regions. Furthermore, both PAS and AcPAS seem to be effective in reducing Mn levels in brain.

Introduction

Manganism is mainly due to occupational exposure to manganese (Mn) (Aschner et al., 2007; Bowler et al., 2006; Crossgrove and Zheng 2004; Myers et al., 2003). Currently, effective clinical treatment options are very limited (Calne et al., 1994; Cook et al., 1974; Ono et al., 2002; Seaton et al., 1999). Para-aminosalicylic acid (PAS, 4-amino-2-hydroxybenzoic acid, Paser; CAS#65-49-6) has been well-known as an anti-tuberculosis drug since the 1950s (Mitnick et al., 2003). The unique structure of PAS, which contains carboxyl and hydroxyl groups, provides the chelating moieties that are essential for Mn binding. Successful treatment of severe chronic manganism with PAS was first reported in two cases of severe Mn poisoning (Ky et al., 1992). A 17-year follow-up study with one of the original patients suggests that PAS therapy needs a long lasting treatment (Jiang et al., 2006). Additional clinical cases, reported mainly in Chinese literature, came to similar conclusions (Shi, 2002; Wu, 1991; Zhao, 1995).

PAS's promising therapeutic effect in the treatment of manganism notwithstanding, its mechanism of action is completely unclear. Some reports have suggested that the effectiveness of PAS in alleviating parkinsonian syndromes is due to its chelating abilities (Zheng et al., 2009). Other studies have showed that PAS may suppress Mn-induced SK-N-MC cell death because of its anti-inflammatory mechanism (Yoon et al., 2009). A recent study revealed that both PAS and EDTA can block Mn toxicity associated with the dopaminergic system; yet the anti-inflammatory agent acetylsalicylic acid does not exhibit a similar effect, leading to the conclusion that the detoxification mechanism of PAS in alleviating Parkinsonism is due primarily to chelation rather than anti-inflammation (Nelson et al., 2010). These mechanistic studies call for a better understanding of the brain distribution, metabolism, and time-

concentration relationships of PAS and its major metabolite, N-acetyl-para-aminosalicylic acid (AcPAS, N-acetyl-4-amino-2-hydroxybenzoic acid; CAS number: 50-86-2) in the targeted brain regions. Surprisingly, the pharmacokinetic behavior of PAS, particularly with regard to its brain distribution, time profiles, and potential cerebral metabolism, remains unknown despite the fact that PAS has a long history of clinical application as an anti-tuberculosis drug. The lack of kinetic knowledge of PAS and its metabolism has hindered the understanding of PAS's effectiveness in clinics as well as the in-depth investigations on its mechanism of action.

To assist the clinical investigations of the efficacy of PAS, we have recently developed a new high-performance liquid chromatographic (HPLC) method to quantify the plasma and tissue concentrations of PAS and AcPAS (Hong et al., 2011). Our preliminary study revealed that PAS can be readily N-acetylated to form N-acetyl-PAS. Following femoral artery injection, both compounds can be detected in blood and brain regions. This finding prompted us to ask what the time courses of PAS and AcPAS are in plasma and brain regions where Mn is known to accumulate, whether PAS or AcPAS is more responsible for Mn chelating, and how the patterns of their brain distribution may relate to the effectiveness of PAS in reducing Mn concentrations in brain. Understandably, a single pharmacokinetic study would not be sufficient to address all these interesting research subjects. Thus, as an initial step towards understanding PAS treatment, we conducted this study in order (1) to determine pharmacokinetic parameters of PAS following intra-arterial injection of PAS so as to fill the gaps in PAS literature, (2) to determine and compare the time dependencies of PAS and AcPAS concentrations in plasma, cerebrospinal fluid (CSF) and selected brain regions following PAS administration, and (3) to determine the pharmacokinetic-pharmacodynamic relationships between PAS and AcPAS by comparing the current results with data from our earlier chelation study (Zheng et al., 2009). The results from

this study will be useful for better designing PAS dosing regimens for clinical uses, future research to explore PAS actions, and more effective drug structures for therapeutic intervention in Mn-induced parkinsonian disorders.

Materials and Methods

Chemicals. Chemicals were obtained from the following sources: PAS, 5-aminosalicylic acid (5-ASA), 2-mercaptoethanol, phenylmethylsulfonyl fluoride (PMSF), polyacrylamide, and tetramethyl-ethylenediamine (TEMED) were purchased from Sigma-Aldrich (St. Louis, MO). AcPAS was synthesized in our laboratory (Hong et al., 2011). HPLC-grade water was prepared using NANOpure Diamond Ultrapure Water Systems (Barnstead International, Dubuque, IA). All reagents were of analytical grade, HPLC grade, or the best available pharmaceutical grade.

Animals. Male Sprague-Dawley rats were purchased from Harlan (Indianapolis, IN) and weighed 250 ± 10 g (mean ± S.D.) at the time of the experiments. The animals were acclimatized for 1 week prior to experimentation in a temperature-controlled, 12/12-hour light/dark room and were allowed free access to water and food. Before the experiment, animals were fasted for 12 hours with free access to distilled, deionized water. The study was conducted in compliance with standard animal use practices and was approved by the Institutional Animal Care and Use Committee at Purdue University.

PAS Administration and biological sample collection. PAS was dissolved in sterile saline daily prior to administration. There were 6 groups for each time point (n=6). For each group, 10 rats were anesthetized with ketamine/xylazine by i.p. injection, followed by PAS injection (200 mg/kg) via the femoral artery. Animals were killed at 0, 5, 15, 30, 45 min, 1, 1.5, 2, 4, and 8 h after dosing. At each time point, CSF samples were first obtained using a 26-gauge butterfly needle (Becton, Dickinson and Company, Franklin Lakes, NJ) inserted between the protuberance and the spine of the atlas and were free of blood. Blood samples were then

collected from the inferior vena cava into a 2-mL heparinized syringe, and an aliquot (200 μL) of the plasma was collected. The rat brain was perfused with saline at a flow rate of 0.8 mL/min through the left common carotid artery. After the 15-min perfusion, the brain was removed from the skull, washed with ice-cold saline, and then placed on an ice-cold filter paper on glass. The choroid plexus, striatum, hippocampus, motor cortex, cerebellum and thalamus, were dissected and homogenized using a homogenization buffer containing 20 mM Tris (pH 7.5), 5 mM EGTA, 1% TritonX-100, 0.1% SDS, 10 μL/mL PMSF, 15 mM 2-mercaptoethanol, and a Protease Inhibitor Cocktail (Calbiochem, San Diego, CA) in a ratio of 1:3 for tissue to buffer. The CSF, plasma and brain homogenates were placed in Eppendorf tubes and immediately frozen at -80^{o}C until analysis. The samples were processed for HPLC analysis within 3 days.

HPLC analysis. The concentrations of PAS and its metabolite AcPAS in plasma and selected brain regions were quantified using a well-established HPLC method developed in this laboratory (Hong et al., 2011). 5-Aminosalicylic acid (5-ASA; CAS number: 89-57-6), a structural analog to PAS, was used as an internal standard (IS). The plasma and tissue samples were thawed at room temperature. One volume (200 μL) was mixed with an equal volume (200 μL) of the internal standard working solution to achieve final IS concentrations of 10.0 μg/mL. The samples were then mixed with an aliquot (300 μL) of methanol, and the pH was adjusted to 1.0 by adding a small volume of 6.0 M hydrochloric acid. After vortex mixing for 1 min, the suspension was centrifuged at 12,000×g for 20 min, dried under nitrogen and reconstructed in 150 μL of the mobile phase. An aliquot (50 μL) of the solution was injected into the HPLC for analysis. All samples were analyzed within the same day of preparation.

A Waters 2695 XE separation module liquid chromatographic system equipped with a built-in autosampler and a Waters 2475 multi λ fluorescence detector was used for separation and

quantification. An excitation wavelength of 337 nm and an emission wavelength of 432 nm were selected for the study. Separation was accomplished using an Econosphere C18 column (5μm, 250 × 4.6 mm) attached to a Spherisorb guard column (5μm, 10 × 4.6 mm). Both the analytical and guard columns were purchased from Alltech (Deerfield, IL). An isocratic mobile phase consisted of methanol and 17.5 mM potassium phosphate buffer, pH 3.5 (equal molar concentration of both monobasic and dibasic potassium salts) was used for separation. Empower Version Build 1154 (Waters Corporation, Milford, MA) was used to collect and analyze the data. Each batch included a freshly prepared standard curve (6 samples between 0.05 and 500 μg/mL) with one quality control sample for every 10 research samples. The method validation was carried out according to the bio-analytical method validation guidance published by the U.S. Food and Drug Administration (Hong et al., 2011). For the protein-binding study, the calibration curve parameters, derived by the statistical analysis of independently prepared seven-point calibration curves of PAS and AcPAS in homogenization buffer, showed an excellent linearity of the assay standards. The assays have been validated for their excellent precision, sensitivity and accuracy on the matrices. The stability study confirmed that there were no stability-related problems during the experiments or the storage of samples.

Protein (tissue) binding study. In vitro plasma or brain protein binding experiments were performed using ultrafiltration. Stock solutions of both compounds were spiked into 1.2 mL of blank plasma samples or brain homogenates to achieve the final concentrations according to the C_{max} values obtained from the plasma or cerebral pharmacokinetic studies. Samples were allowed to equilibrate in a water-bath shaker at 37^{o}C for 1 h. An aliquot (0.5 mL) was collected for determination of total drug concentration according to the HPLC procedure described above. A second aliquot (0.5 mL) of plasma or brain sample was added to a Microcon ultrafiltration

system (Millipore, America) with a membrane molecular weight cutoff at 30kDa. The system was centrifuged at 1500×g for 15 min, and a small volume (less than 0.1 mL) of filtrate was used for HPLC analysis of free, unbound drug concentrations. The free, unbound fraction of drug was calculated as the ratio of drug concentration in the filtrate to that in plasma or brain homogenate prior to ultrafiltration. Nonspecific membrane binding was estimated by dissolving the tested compounds in protein-free homogenization buffer, conducting ultrafiltration without incubation under the same experimental conditions, and quantifying drug concentrations in both unfiltered and filtrated samples by HPLC.

Pharmacokinetic and statistical analyses. The concentration-time profiles of PAS and AcPAS in plasma, CSF, and brain tissues were analyzed by non-compartmental methods using software DAS version 2.0.1 (Mathematical Pharmacology, Professional Committee of China, Shanghai, China). Values of C_{max} and T_{max} were obtained directly from concentration-time profiles.

All data are presented as mean ± SD. Statistical analysis for comparison of two means was performed using one-way ANOVA with post hoc comparisons by the Dunnett's tests (Kaleidagraph 3.6). In all cases, a probability level of p-value < 0.05 was considered as the criterion of significance.

Results

Pharmacokinetics of PAS and AcPAS in blood and CSF. After femoral artery injection of PAS (200 mg/kg) in Sprague-Dawley rats, the concentration-time profile of PAS in plasma followed a multi-exponential equation:

$$C(t)_{PAS} = 5160.0e^{-1.04t} + 442.2e^{-0.02t} \quad (R^2=0.999).$$

In general, PAS was rapidly eliminated from the plasma with an initial fast phase between 0 and 1.5 h and a slow terminal phase between 1.5 and 2 h (Fig. 1A). The terminal elimination $t_{1/2}$ of PAS was 34 min. By 4 h, PAS concentrations in plasma were nearly undetectable. In contrast, the concentration of AcPAS, a major metabolite of PAS, rose slowly, yet steadily, in plasma and reached the C_{max} at 86 min after PAS administration (Fig. 1A). The area under curve ($AUC_{0-\infty}$) of the parent PAS in plasma was about 3-fold greater than that of AcPAS (Table 1).

In the CSF, PAS concentrations rose rapidly and reached the C_{max} at 17 min following injection of PAS (Fig. 1B). Interestingly, the CSF profile of AcPAS reached the C_{max} at 44 min. The $AUC_{0-\infty}$ of CSF PAS was about 7.5-fold greater than that of AcPAS in the CSF. The results suggest that PAS rapidly distributed from the blood compartment into the CSF compartment and the metabolite AcPAS in the CSF seemed likely to result from AcPAS present in the blood and/or AcPAS formed in the brain.

Pharmacokinetics of PAS and AcPAS in selected brain regions. Following administration of PAS, the highest tissue concentrations of PAS and AcPAS were reached in the

DMD Fast Forward. Published on July 18, 2011 as DOI: 10.1124/dmd.111.040915
This article has not been copyedited and formatted. The final version may differ from this version.

choroid plexus (Fig. 2A). The C_{max} of PAS in the choroid plexus was about 3.6-fold higher than that in the CSF but about 12 to 19-fold higher than in the other brain regions examined (Table 1). While the T_{max} in the choroid plexus was 29 min, the T_{max} values in the striatum (Fig. 2B), hippocampus (Fig. 2C) or motor cortex (Fig. 2D) were between 42 and 72 min, indicating a lag-time for PAS to reach these brain regions with choroid plexus the earliest and striatum the latest tissues to reach their maximums. Noticeably, the tissue PAS levels reached C_{max} rapidly in cerebellum (5 min) (Fig. 2E) and thalamus (15 min) (Fig. 2F) and quickly declined thereafter. It has been reported in the literature that both cerebellum and thalamus are brain regions with abundant blood flow from the cerebral vascular including the posterior cerebral arteries (Rhoton, 2007; Schmahmann, 2003).

Following the administration of PAS, the metabolite AcPAS displayed distinct kinetic characteristics in brain regions. The $t_{1/2}$s of AcPAS in most brain regions tended to be longer than those of PAS in the same brain regions (Table 1). Except for the choroid plexus, the $AUC_{0-\infty}$ and C_{max} values of AcPAS in most brain regions were significantly higher than those of the parent PAS (Fig. 2B-F; Table 1). Typically, striatum exhibited the greatest ratio of $C_{max(AcPAS)}/C_{max(PAS)}$ with a value of 2.51, and hippocampus had the highest $AUC_{(AcPAS)}$ $/AUC_{(PAS)}$ ratio with a value of 5.07. (3) By normalizing the brain regional $AUC_{0-\infty}$ to the corresponding plasma $AUC_{0-\infty}$ of PAS or AcPAS, it became evident that the tissue to plasma $AUC_{0-\infty}$ ratios of PAS were significantly lower than those of AcPAS in all six brain regions (Fig. 3).

Plasma Protein and Brain Tissue Binding. The higher tissue concentrations of AcPAS compared to PAS prompted us to ask whether PAS had a higher protein binding capability than AcPAS in plasma. To test this hypothesis, we conducted protein binding experiments to

determine the free, unbound PAS and AcPAS levels in plasma and 6 selected brain regions following ultrafiltration and adjusted for nonspecific filter membrane binding. Our data showed that a very high percentage (>90%) of the PAS molecules existed in the free, unbound state, whereas the unbound AcPAS fractions were between 80 and 87% (Table 2). Both PAS and AcPAS appeared to exist in plasma and brain tissues mainly in the free, unbound form. AcPAS exhibited higher plasma and tissue binding than PAS did.

Tissue levels of PAS/AcPAS and their efficacy in Mn chelation. Our previous results have shown that treatment of Mn-exposed rats with PAS leads to reduced Mn concentrations in rat brains (Zheng et al., 2009). To understand whether this is due to PAS or its metabolite AcPAS, we calculated the percent reduction in Mn concentrations in brain regions after the rats received ip injection of PAS at a dose of 200 mg/kg for 3 weeks (Zheng et al., 2009) and correlated the reduction percentage with the $AUC_{0-\infty}$ of either PAS or AcPAS in the same regions (Table 1). Linear regression analysis revealed that the percentage of Mn reduction in brain regions was better correlated with the $AUC_{0-\infty}$ values of AcPAS (p-value < 0.05) than those of PAS (p-value > 0.05) (Fig. 4). Interestingly, it was noticed that the brain region where the metabolite AcPAS was detected at the higher level (e.g., hippocampus, striatum, and thalamus) were the regions where Mn levels were reduced more effectively following PAS treatment. It is possible that both PAS and AcPAS may play roles in reducing tissue accumulations of Mn with AcPAS being more effective than PAS, although other mechanisms should not be excluded.

DMD Fast Forward. Published on July 18, 2011 as DOI: 10.1124/dmd.111.040915
This article has not been copyedited and formatted. The final version may differ from this version.

Discussion

PAS has been used in clinics as the secondary choice for the treatment of tuberculosis since the 1950's (Mitnick et al., 2003). To our surprise, its cerebral pharmacokinetic behavior remains unknown. Thus, the study presented in this report was intended to fill the gaps with regard to the pharmacokinetics and brain distribution of PAS in a rat model. The plasma kinetics of PAS show the following characteristics. First, PAS, upon intra-arterial injection, was rapidly eliminated from the blood compartment and rapidly entered the CSF, cerebellum and thalamus. Second, among the brain tissues studied, the choroid plexus contained the highest PAS concentration, about 10 to 20-fold higher than other regions. Most of PAS molecules were present as free, unbound PAS in plasma, CSF and brain tissues. Third, PAS was extensively metabolized to form AcPAS; the latter reached higher brain tissue concentrations and possessed a longer $t_{1/2}$ than the parent PAS did. Finally, the concentrations of PAS and its metabolite AcPAS appeared to be associated directly with PAS's efficacy in reducing the tissue burden of Mn.

The finding of a fast elimination of PAS in plasma and brain tissues supports the clinical observation that high PAS doses are required to achieve effective therapeutic outcomes (Jiang et al., 2006). This observation is also consistent with our previous animal results that indicated that a high dose of PAS (200 mg/kg) acts far more effectively than low doses of PAS in reducing Mn levels in brain tissues (Zheng et al., 2009). The relatively short $t_{1/2}$ may not allow sufficient PAS to pass across the brain barriers to achieve effective therapeutic concentrations in the brain areas where Mn ions accumulate. Our results are also consistent with the current practice in clinics of administering PAS daily via iv infusions rather than administering a single dose injection or oral

DMD Fast Forward. Published on July 18, 2011 as DOI: 10.1124/dmd.111.040915
This article has not been copyedited and formatted. The final version may differ from this version.

dose to manganism patients (Jiang et al., 2006). Clearly a constant high blood level of PAS achieved by iv infusion allows drug molecules to distribute to the targeted brain regions. It is known that Mn preferentially accumulates in the choroid plexus, striatum, and hippocampus (Lai et al., 1999; Li et al., 2006; Reaney et al., 2006; Roels et al., 1997; Zheng et al., 1999, 2009). This was also proven true by comparing the current kinetic data with our earlier chelating experiments (Zheng et al., 2009), since brain regions having high PAS and AcPAS concentrations were the regions in which PAS therapy exerted maximal reductions of Mn.

The question is whether PAS or its major metabolite AcPAS, is the essential molecule in removing Mn from the brain. Recent studies suggested that the action of PAS in alleviating Parkinsonism is more likely related to its chelating abilities than its anti-inflammatory properties (Nelson et al., 2010; Zheng et al., 2009). Since both PAS and AcPAS contain carboxyl and hydroxyl groups, these unique structural properties confer both molecules with the essential moieties to chelate Mn. From the kinetic point of view, however, the tissue C_{max} and $AUC_{0-\infty}$ of the metabolite AcPAS were much greater than those of parent PAS. Thus, it is tempting to postulate that AcPAS may play a more important role than PAS in chelating and mobilizing Mn from the brain. This conjecture, however, requires further studies, such as the determination of in vitro dissociation constants between the two drug molecules and Mn and experiments in which the compounds and Mn are administered to animals, to directly compare the two compounds.

Our results clearly indicate that the AcPAS concentration is much higher than that of PAS in local brain regions. Several factors may contribute to the higher tissue level of AcPAS, including faster influx transport by brain barriers and/or slower efflux clearance from the brain. Furthermore, the lower water solubility or higher lipophilicity may allow AcPAS molecules to cross the brain barriers via the passive diffusion more readily than does PAS. On the other hand,

AcPAS has a stronger tissue binding affinity with brain tissue protein. Upon reaching the brain regions where Mn accumulates, the higher tissue binding of AcPAS may allow the AcPAS to be eliminated by brain barrier systems and spinal cord more slowly than PAS, although both PAS and AcPAS are present mainly in the free, unbound form.

The high tissue concentration of AcPAS could also be due to the conversion of PAS to AcPAS by arylamine N-acetyltransferases. Results from our own studies (Hong et al., 2011) and human studies by other laboratories (Dupret et al., 1994; Goodfellow et al., 2000) have established that arylamine N-acetyltransferase is capable of metabolizing PAS to AcPAS. The metabolism could happen in plasma and liver, and AcPAS in brain could be the result of the AcPAS in the blood diffusing into the brain. This may be the case for AcPAS in the CSF and choroid plexus since the time profiles of AcPAS in the CSF and choroid plexus paralleled those of plasma AcPAS. However, when the time profiles of striatum, hippocampus, cortex, cerebellum and thalamus were compared with those of AcPAS in plasma, it became clear that AcPAS in these brain regions had a rather sharp increase which is distinctly different from the pattern of the plasma AcPAS. Thus, it is reasonable to suggest that PAS may be biotransformed to AcPAS either by cerebral endothelial cells that constitute the blood-brain barrier or by brain cells in the targeted area, or both. The presence of arylamine N-acetyltransferase has indeed been demonstrated in mouse brain regions including the cortex and cerebellum (Sugamori et al., 2003).

Finally, the high level of AcPAS in brain tissues could also be due to an ineffective clearance of the molecules by the efflux-transport systems expressed at brain barriers (Zheng et al., 2003). P-glycoprotein at the blood-brain barrier, for example, has been shown to exclude endogenous and exogenous compounds from brain parenchyma (Sun et al., 2003). It is unclear if

P-glycoprotein transports PAS or AcPAS back into the blood or whether it has a unique preference for one molecule over the other. The low concentration of PAS in parenchyma could be due to the highly efficient clearance of PAS from the brain interstitial fluid back into the blood by efflux transporter(s). P-Glycoprotein is also expressed at the apical side of rat choroid plexus (Daood et al., 2008; Loscher and Potschka, 2005; Sun et al., 2003). It is possible that it may regulate the influx of PAS and/or AcPAS into the epithelial cells of the choroid plexuses (the blood-CSF barrier). The exact nature of the transport of these molecules by brain barrier systems is an interesting research subject for future in-depth investigations.

In summary, this pharmacokinetic study suggests that PAS has a short plasma $t_{1/2}$ and is capable of rapidly distributing to the CSF. PAS can be metabolized to AcPAS, which has much higher tissue concentrations and possesses a longer $t_{1/2}$ than its parent PAS. Both PAS and AcPAS are present in blood and tissues as free, unbound molecules. The concentrations of PAS and AcPAS appeared to be associated with Mn reduction in cerebral tissues.

Acknowledgments

The authors would like to thank Xue Fu, Yanshu Zhang and Andrew Monnot for their technical assistance during this study and Professor Gary Carlson for proofreading of this manuscript.

Authorship Contributions

Participated in research design: LH; WZ; SZ; YMJ

Conducted experiments: LH; WJ

Contributed new reagents or analytic tools: None

Performed data analysis: LH; HP; WZ

Wrote or contributed to the writing of the manuscript: LH; WZ; SZ

References

Aschner M, Guilarte TR, Schneider JS, and Zheng W (2007) Manganese: recent advances in understanding its transport and neurotoxicity. *Toxicol Appl Pharmacol* **221**: 131-147.

Bowler RM, Gysens S, Diamond E, Nakagawa S, Drezgic M, and Roels HA (2006) Manganese exposure: neuropsychological and neurological symptoms and effects in welders. *Neurotoxicology* **27**: 315-326.

Calne DB, Chu NS, Huang CC, Lu CS, and Olanow W (1994) Manganism and idiopathic parkinsonism: similarities and differences. *Neurology* **44**: 1583-1586.

Cook DG, Fahn S, and Brait KA (1974) Chronic manganese intoxication. *Arch Neurol* **30**: 59-64.

Crossgrove J and Zheng W (2004) Manganese toxicity upon overexposure. *NMR Biomed* **17**: 544-553.

Daood M, Tsai C, Ahdab-Barmada M, and Watchko JF (2008) ABC transporter (P-gp/ABCB1, MRP1/ABCC1, BCRP/ABCG2) expression in the developing human CNS. *Neuropediatrics* **39**: 211-218.

Dupret JM, Goodfellow GH, Janezic SA, and Grant DM (1994) Structure-function studies of human arylamine N-acetyltransferases NAT1 and NAT2. Functional analysis of recombinant NAT1/NAT2 chimeras expressed in Escherichia coli. *J Biol Chem* **269**: 26830-26835.

Goodfellow GH, Dupret JM, and Grant DM (2000) Identification of amino acids imparting acceptor substrate selectivity to human arylamine acetyltransferases NAT1 and NAT2. *Biochem J* **348**: 159-166.

Hong L, Jiang W, Zeng S, and Zheng W (2011) HPLC analysis of para-aminosalicylic acid and its metabolite in plasma, cerebrospinal fluid and brain tissues. *J Pharm Biomed Anal* **54**: 1101-1109.

Jiang YM, Mo XA, Du FQ, Fu X, Zhu XY, Gao HY, Xie JL, Liao FL, Pira E, and Zheng W (2006) Effective treatment of manganese-induced occupational Parkinsonism with p-aminosalicylic acid: a case of 17-year follow-up study. *J Occup Environ Med* **48**: 644-649.

Ky SQ, Deng HS, Xie PY, and Hu W (1992) A report of two cases of chronic serious manganese poisoning treated with sodium para-aminosalicylic acid. *Br J Ind Med* **49**: 66-69.

Lai JC, Minski MJ, Chan AW, Leung TK, and Lim L (1999) Manganese mineral interactions in brain. *Neurotoxicology* **20**: 433-444.

Li GJ, Choi BS, Wang X, Liu J, Waalkes MP, and Zheng W (2006) Molecular mechanism of distorted iron regulation in the blood-CSF barrier and regional blood-brain barrier following in vivo subchronic manganese exposure. *Neurotoxicology* **27**: 737-744.

Loscher W and Potschka H (2005) Role of drug efflux transporters in the brain for drug disposition and treatment of brain diseases. *Prog Neurobiol* **76**: 22-76.

Mitnick C, Bayona J, Palacios E, Shin S, Furin J, Alcantara F, Sanchez E, Sarria M, Becerra M, Fawzi MC, Kapiga S, Neuberg D, Maguire JH, Kim JY, and Farmer P (2003) Community-based therapy for multidrug-resistant tuberculosis in Lima, Peru. *N Engl J Med* **348**: 119-128.

Myers JE, Thompson ML, Ramushu S, Young T, Jeebhay MF, London L, Esswein E, Renton K, Spies A, Boulle A, Naik I, Iregren A, and Rees DJ (2003) The nervous system effects of

occupational exposure on workers in a South African manganese smelter. *Neurotoxicology* **24**: 885-894.

Nelson M, Huggins T, Licorish R, Carroll MA, and Catapane EJ (2010) Effects of p-Aminosalicylic acid on the neurotoxicity of manganese on the dopaminergic innervation of the cilia of the lateral cells of the gill of the bivalve mollusc, Crassostrea virginica. *Comp Biochem Physiol C Toxicol Pharmacol* **151**: 264-270.

Ono K, Komai K, and Yamada M (2002) Myoclonic involuntary movement associated with chronic manganese poisoning. *J Neurol Sci* **199**: 93-96.

Reaney SH, Bench G, and Smith DR (2006) Brain accumulation and toxicity of Mn(II) and Mn(III) exposures. *Toxicol Sci* **93**: 114-124.

Rhoton AL, Jr. (2007) The cerebrum. Anatomy. *Neurosurgery* **61:** 37-118.

Roels H, Meiers G, Delos M, Ortega I, Lauwerys R, Buchet JP, and Lison D (1997) Influence of the route of administration and the chemical form (MnCl2, MnO2) on the absorption and cerebral distribution of manganese in rats. *Arch Toxicol* **71**: 223-230.

Schmahmann JD (2003) Vascular syndromes of the thalamus. *Stroke* **34:** 2264-2278.

Seaton CL, Lasman J, and Smith DR (1999) The effects of CaNa(2)EDTA on brain lead mobilization in rodents determined using a stable lead isotope tracer. *Toxicol Appl Pharmacol* **159**: 153-160.

Shi XY (2002) One case on chronic serious manganism treated with sodium para-aminosalicylic acid [in Chinese]. *J Baotou Medical College* **18**: 161.

Sugamori KS, Wong S, Gaedigk A, Yu V, Abramovici H, Rozmahel R, and Grant DM (2003) Generation and functional characterization of arylamine N-acetyltransferase Nat1/Nat2 double-knockout mice. *Mol Pharmacol* **64**: 170-179.

Sun H, Dai H, Shaik N, and Elmquist WF (2003) Drug efflux transporters in the CNS. *Adv Drug Deliv Rev* **55**: 83-105.

Wu P (1991) A report of one case on the diagnostic treatment with PAS-Na [in Chinese]. *Ind Health Occup Dis* **17**: 163.

Yoon H, Kim DS, Lee GH, Kim JY, Kim DH, Kim KW, Chae SW, You WH, Lee YC, Park SJ, Kim HR, and Chae HJ (2009) Protective effects of sodium para-amino salicylate on manganese-induced neuronal death: the involvement of reactive oxygen species. *J Pharm Pharmacol* **61**: 1563-1569.

Zheng W, Jiang YM, Zhang Y, Jiang W, Wang X, and Cowan DM (2009) Chelation therapy of manganese intoxication with para-aminosalicylic acid (PAS) in Sprague-Dawley rats. *Neurotoxicology* **30**: 240-248.

Zheng W, Zhao Q, Slavkovich V, Aschner M, and Graziano JH (1999) Alteration of iron homeostasis following chronic exposure to manganese in rats. *Brain Res* **833**: 125-132.

Zheng W, Aschner M, and Ghersi-Egea JF (2003) Brain barrier systems: a new frontier in metal neurotoxicological research. *Toxicol Appl Pharmacol* **192**: 1-11

Zhao DF (1995) The Clinical Observation on manganism treated with PAS-Na [in Chinese]. *J Guiyang Medical College* **20**: 327.

Footnotes

This work was supported in part by U.S. National Institute of Health/National Institute of Environmental Health Sciences [Grant RO1 ES008146], U.S. Department of Defense Contract [USAMRMC W81XWH-05-1-0239], and the National Major Special Project for Science and Technology Development, Ministry of Science and Technology of China [Grant 2009ZX09304-003].

Figure Legends

FIG. 1. Concentration-time profiles of PAS and AcPAS in body fluids. The rats received single femoral artery injections of PAS at 200 mg/kg. At the times indicated, animals (*n*=6) were anesthetized, and CSF and blood were collected for quantification of PAS and AcPAS. (A). PAS and AcPAS in plasma. (B). PAS and AcPAS in CSF. Data represent Mean $\pm$ S.D.

FIG. 2. Concentration-time profiles of PAS and AcPAS in selected brain regions. The rats received single femoral artery injections of at 200 mg/kg. At the times indicated, animals (*n*=6) were anesthetized, and brain tissues were dissected for quantification of PAS and AcPAS. (A). PAS and AcPAS in choroid plexus. (B). PAS and AcPAS in striatum. (C). PAS and AcPAS in hippocampus. (D). PAS and AcPAS in motor cortex. (E). PAS and AcPAS in cerebellum. (F). PAS and AcPAS in thalamus. Data represent Mean $\pm$ S.D.

FIG. 3. Ratios of brain/CSF $AUC_{0-\infty}$ of PAS or AcPAS versus respective plasma $AUC_{0-\infty}$ of PAS or AcPAS. Data represent Mean $\pm$ S.D., *n*=6. ***: $p<0.0001$ compared between PAS and AcPAS.

FIG. 4. Linear regression analysis of the association between brain $AUC_{0-\infty}$ and percentage of Mn reduction in brain regions (%) following PAS treatment. (A). PAS $AUC_{0-\infty}$ and % Mn reduction. (B). AcPAS $AUC_{0-\infty}$ and % Mn reduction. The % Mn reduction data are derived from the report by Zheng et al. (Zheng et al., 2009). CP: choroid plexus; CB: cerebellum; MC: motor cortex; HP: hippocampus; ST: striatum; and TH: thalamus.

DMD Fast Forward. Published on July 18, 2011 as DOI: 10.1124/dmd.111.040915
This article has not been copyedited and formatted. The final version may differ from this version.

TABLE 1
Pharmacokinetic parameters of PAS and AcPAS in rat plasma, CSF and brain regions

	Analyte	$AUC_{0-\infty}$ (μg•min/g)	C_{max} (μg/g)	$t_{1/2}$ (min)	T_{max} (min)	MRT (min)
Plasma	PAS	24914±492.9	431.0±7.6	34.1±0.6	4.7±0.5	51.1±1.1
	AcPAS	8336.3±120.4	52.7±3.2	147.2±8.6	86. 3±15.0	205.1±11.9
CSF	PAS	1572.8±112.1	11.9±0.8	99.1±11.3	17.2±4.1	146.9±15.1
	AcPAS	207.8±25.7	2.3±0.5	75.2±40.4	44.0±3.1	124.9±36.5
Choroid Plexus	PAS	3483.0±410.6	42.8±4.9	42.7±8.8	29.2±3.3	73.9±12.3
	AcPAS	2239.3±183.2	30.7±3.5	48.6±4.6	31.3±4.1	84.4±3.0
Striatum	PAS	673.1±41.5	2.2±0.3	174.6±16.0	72.3±2.0	287.8±22.2
	AcPAS	836.5±13.1	5.4±0.3	101.0±9.6	53.5±6.4	134.0±6.3
Hippocampus	PAS	239.8±49.6	3.0±0.2	77.3±39.2	44.0±3.1	119.0±43.9
	AcPAS	1215.8±83.9	6.4±0.3	111.8±10.5	45.7±5.5	173.9±12.6
Motor cortex	PAS	274.7±40.2	3.2±0.4	54.2±30.7	42.3±5.1	92.1±33.3
	AcPAS	619.5±24.1	5.1±0.4	81.6±9.7	44.0±3.1	128.2±10.3
Cerebellum	PAS	291.3±47.8	3.6±0.2	67.7±15.7	4.8±0.8	94.2±21.9
	AcPAS	1068.0±29.1	3.8±0.3	180.5±8.1	40.8±9.5	272.9±9.5
Thalamus	PAS	215.2±38.0	2.6±0.4	97.1±38.4	15.0±2.0	129.2±48.2
	AcPAS	933.9±126.1	4.0±0.4	139.5±37.2	48.5±5.1	216.0±51.9

Data represent Mean ± S.D., *n*=6.

DMD Fast Forward. Published on July 18, 2011 as DOI: 10.1124/dmd.111.040915
This article has not been copyedited and formatted. The final version may differ from this version.

TABLE 2
Brain tissue protein binding of PAS and AcPAS

Plasma/Tissues	PAS		AcPAS	
	Concentration (μg/g)	$F_{unbound}$ (%)	Concentration (μg/g)	$F_{unbound}$ (%)
Plasma (μg/mL)	431.00	102.4±3.2	52.70	80.7±2.2 **
Choroid Plexus	42.81	91.5±8.0	30.70	86.8±5.0
Striatum	2.17	93.0±4.0	5.44	80.3±2.0 *
Hippocampus	3.04	99.1±4.3	6.36	85.3±2.5 *
Motor Cortex	3.24	101.3±3.0	5.10	82.0±1.7 **
Cerebellum	3.57	102.8±5.6	3.75	81.5±3.1 *
Thalamus	2.63	98.5±4.5	4.02	84.2±2.8 *

$F_{unbound}$: fraction unbound. Data represent Mean ± S.D., *n*=5. *: p<0.001; **: p<0.0001 as compared to PAS.

Figure. 1A

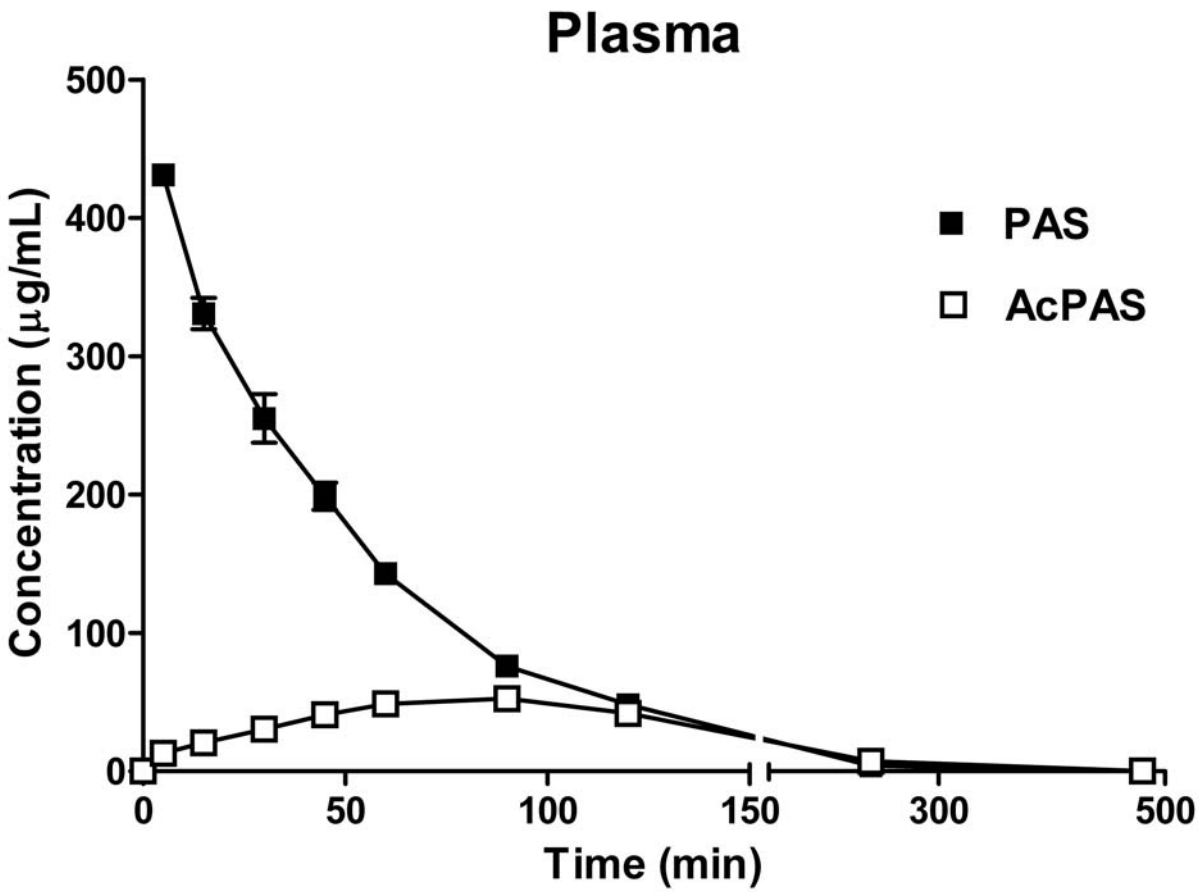

Figure. 1B

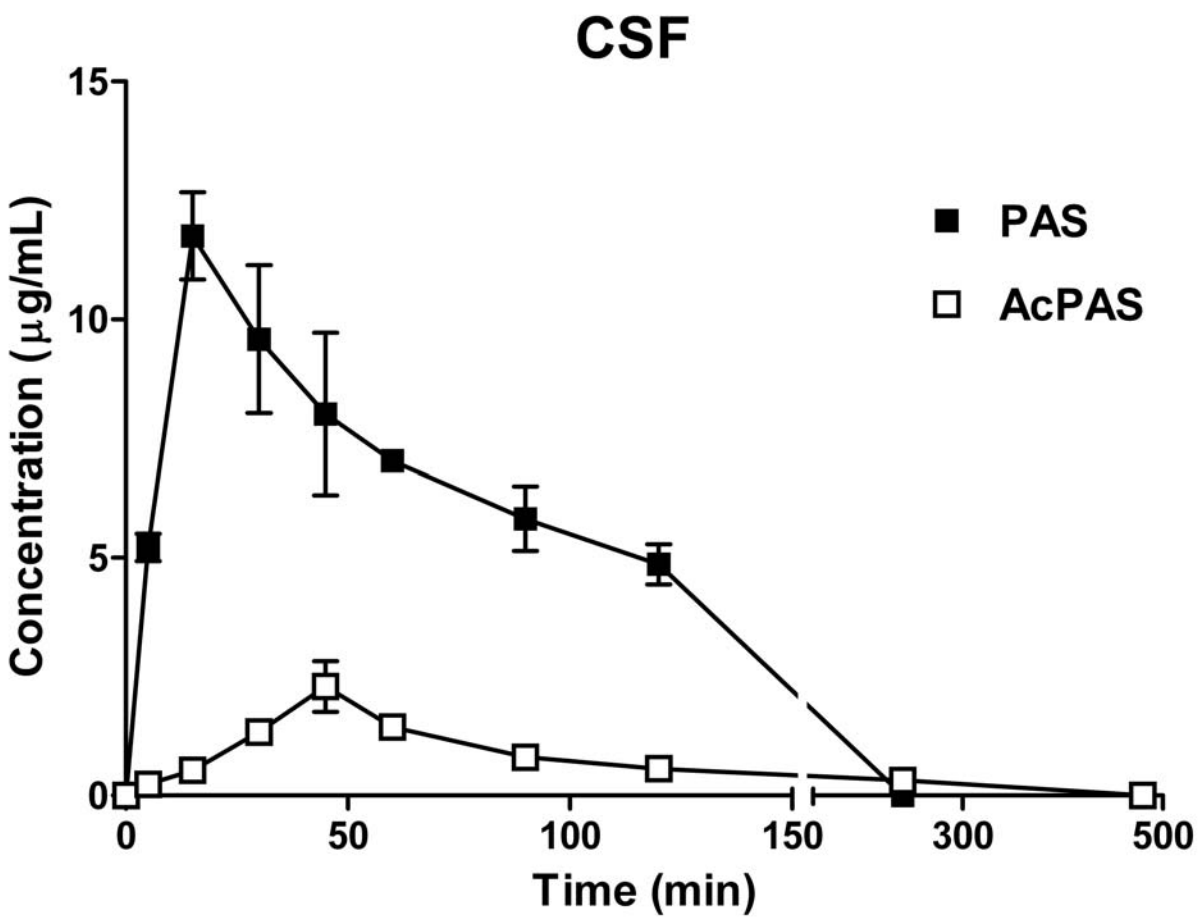

Figure. 2A

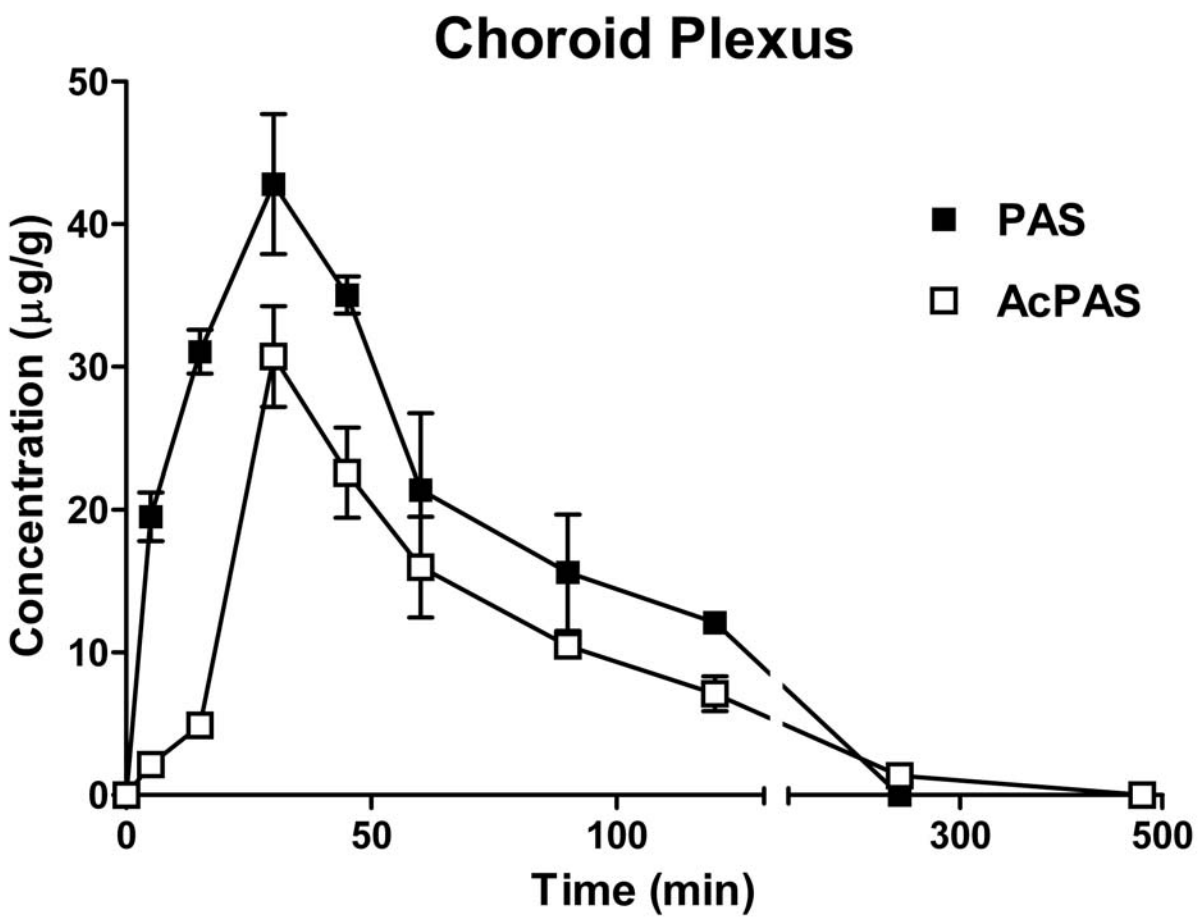

Figure. 2B

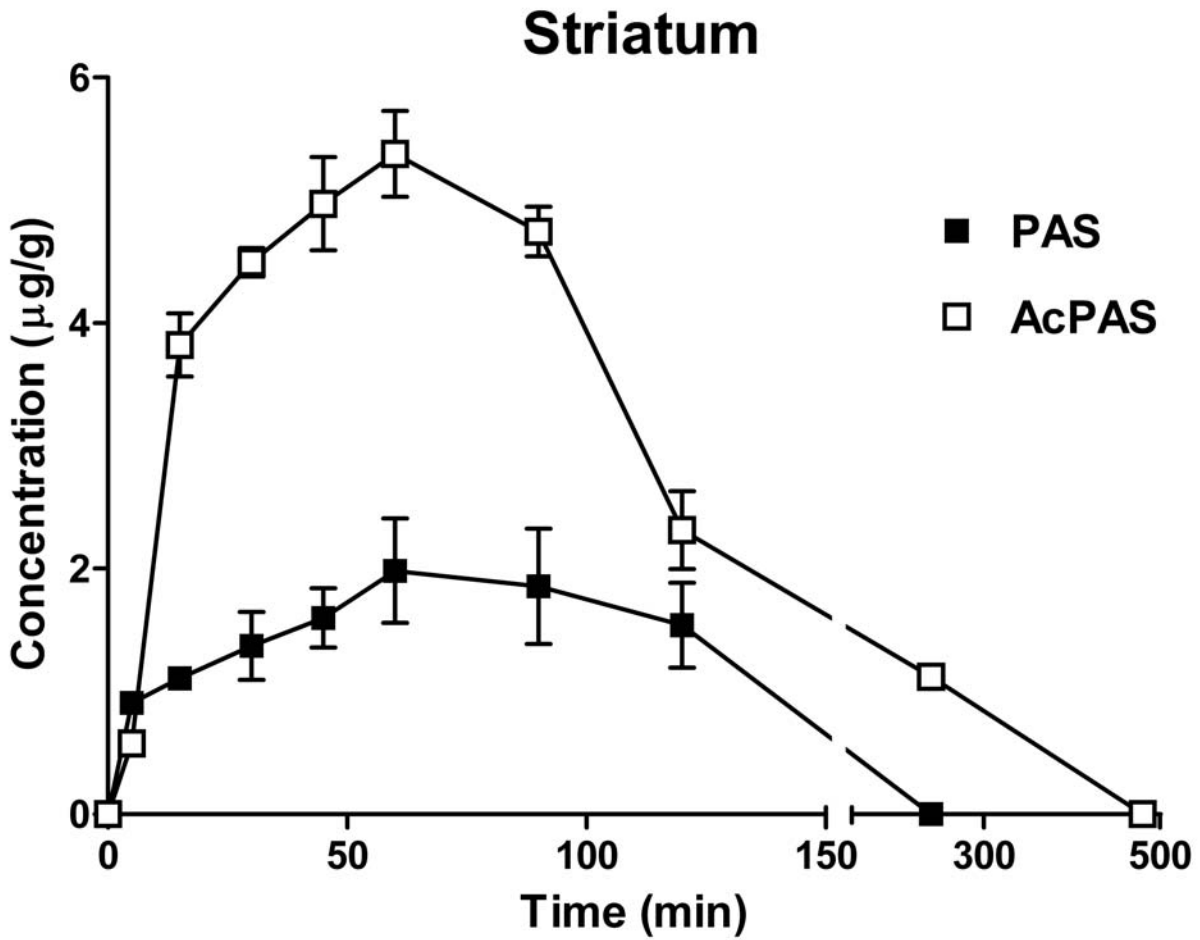

Figure. 2C

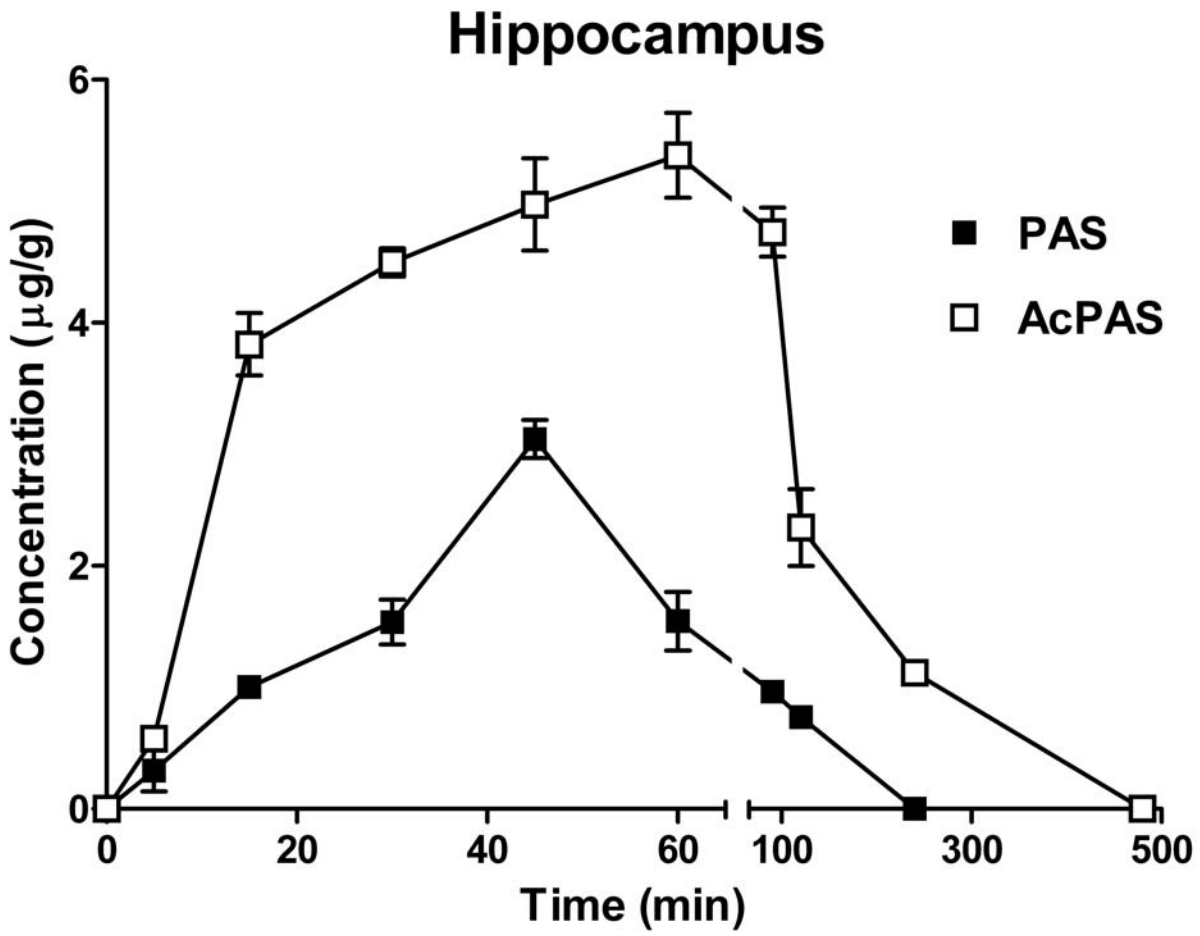

Figure. 2D

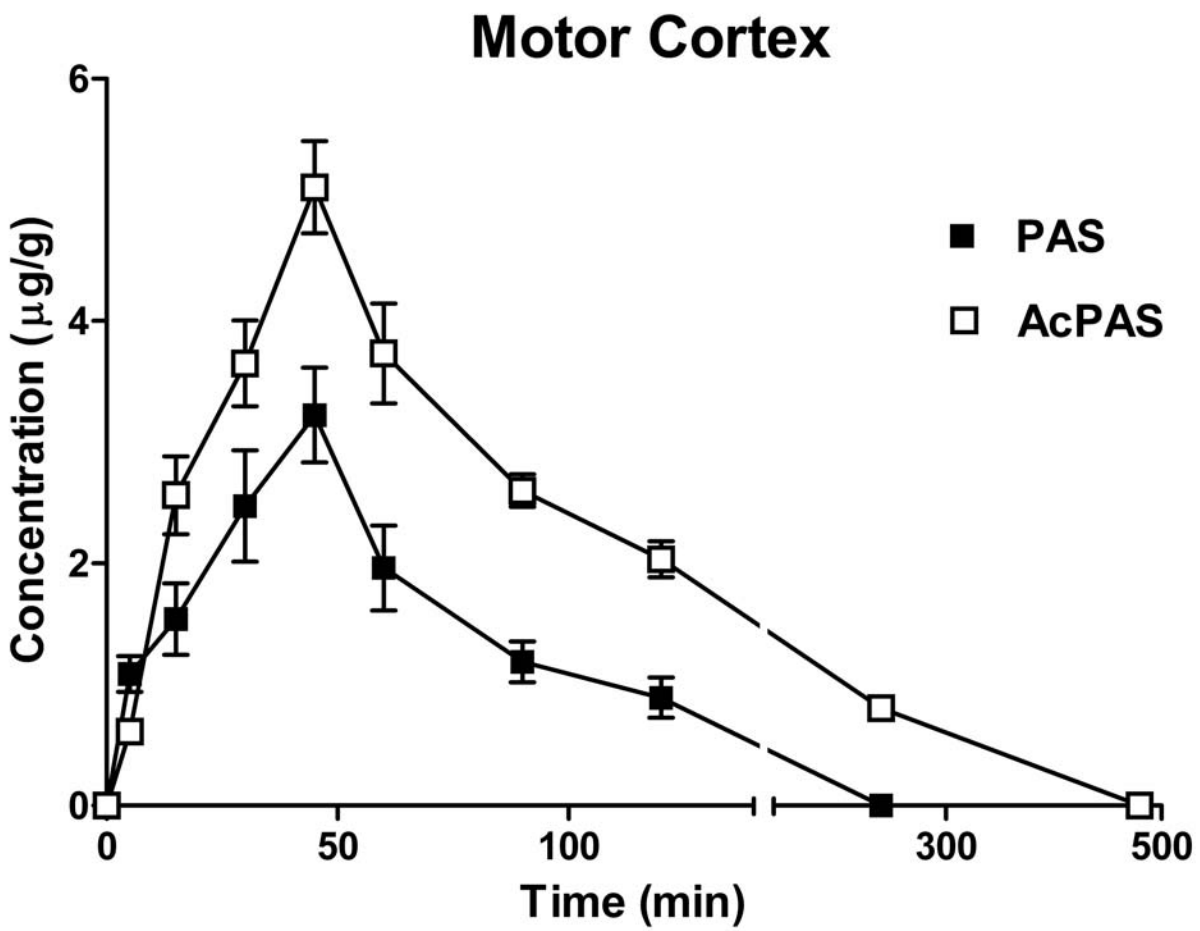

Figure. 2E

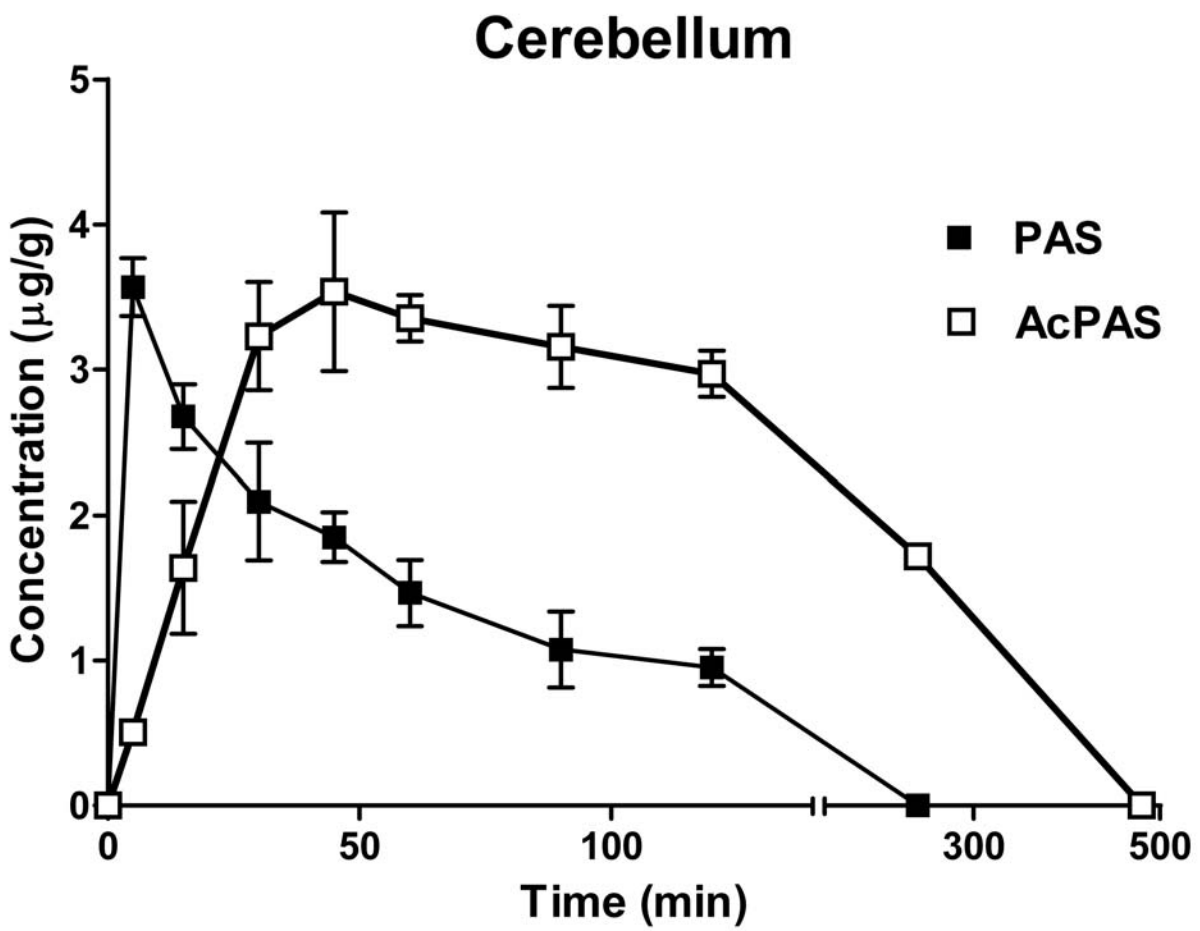

Figure. 2F

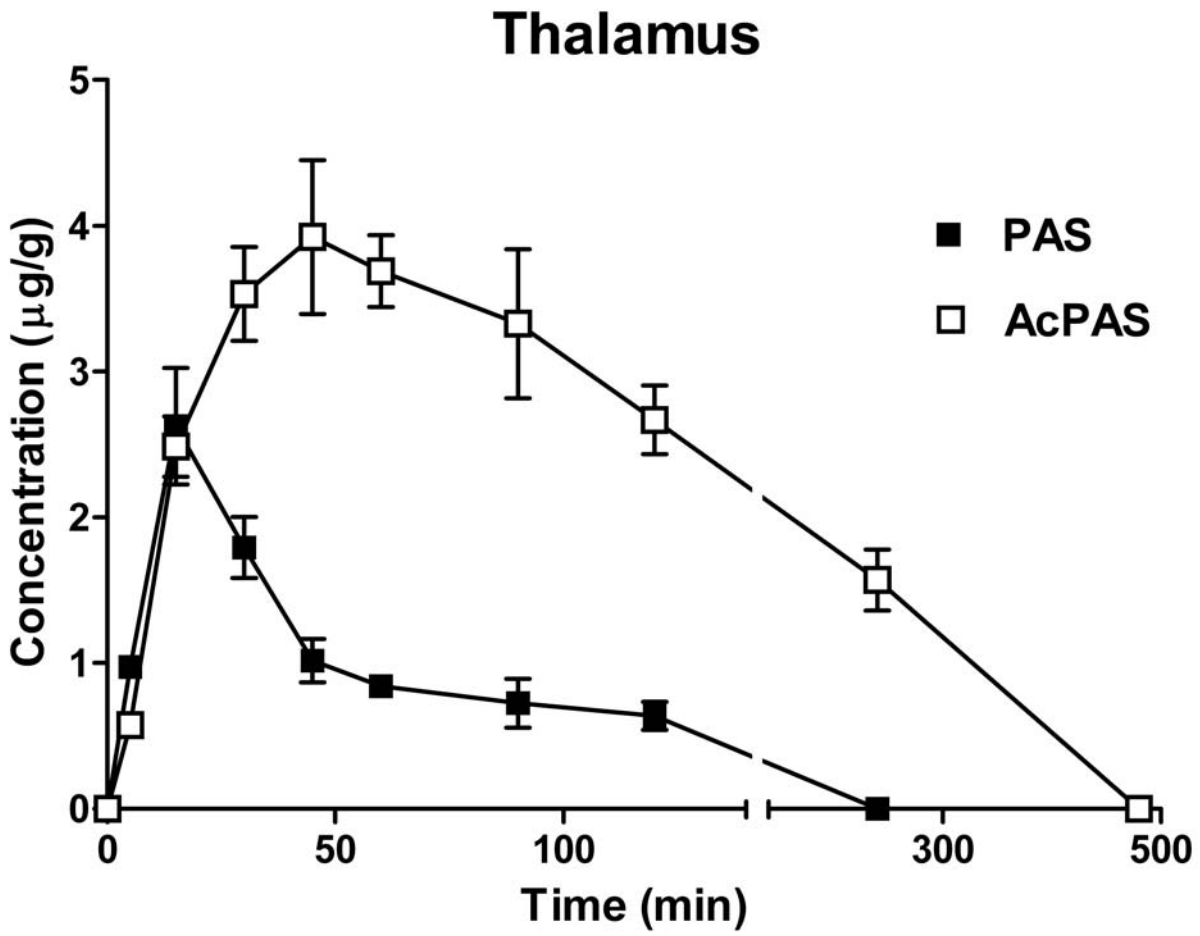

Figure. 3

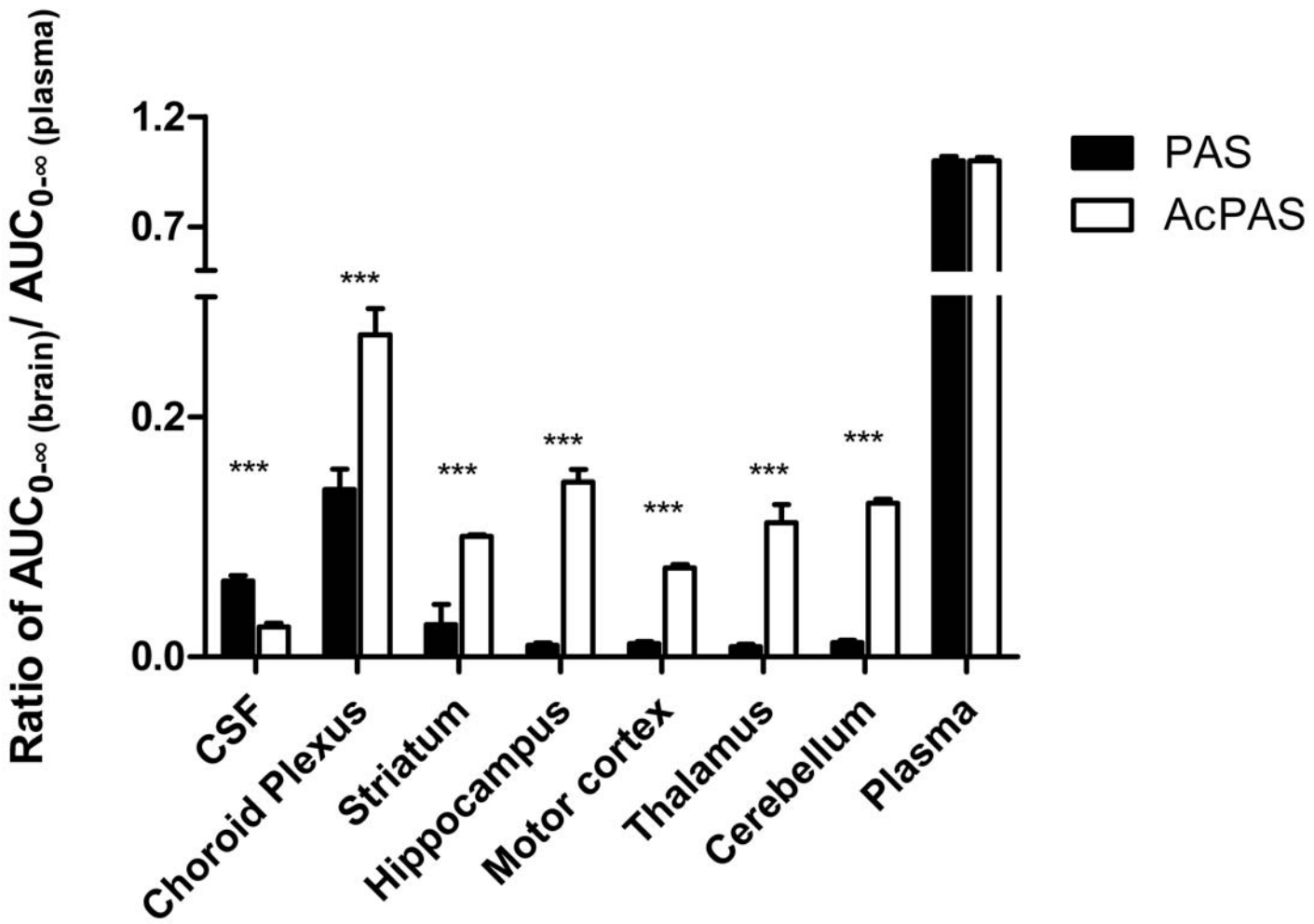

Figure. 4A

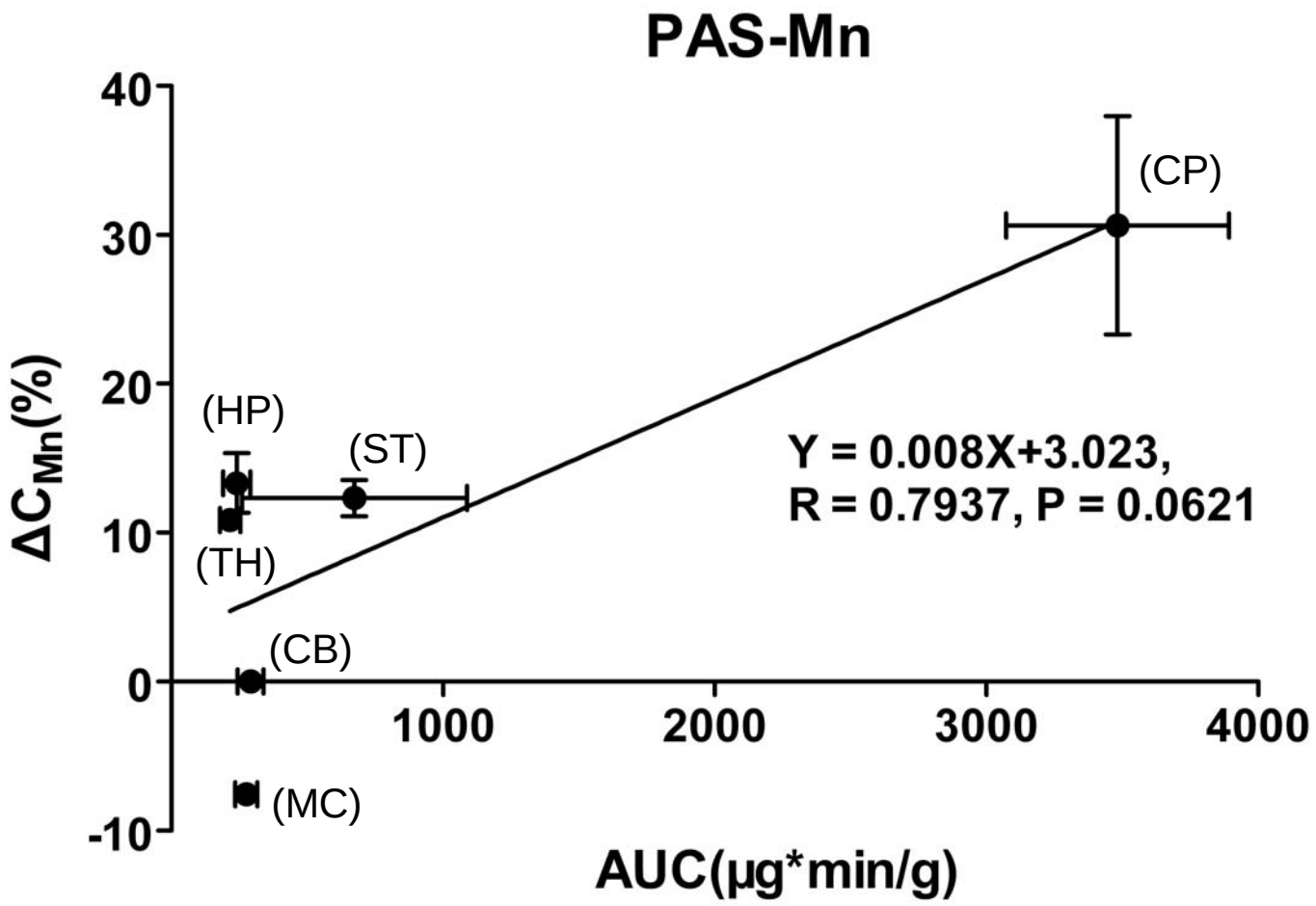

Figure. 4B